The Canadian Mineralogist
Vol. 46, pp. 1577-1591 (2008)
DOI: 10.3749/canmin.46.5.1577

INCREASE IN Al–Si AND Na–Ca DISORDER WITH TEMPERATURE IN SCAPOLITE $Me_{32.9}$

SYTLE M. ANTAO[§]

Advanced Photon Source, Argonne National Laboratory, Argonne, Illinois 60439, USA

ISHMAEL HASSAN

Department of Chemistry, University of the West Indies, Mona, Kingston 7, Jamaica

ABSTRACT

Scapolite $Me_{32.9}$ (marialite) from Monmouth Township, Ontario, was studied using *in situ* synchrotron powder X-ray diffraction (XRD) and Rietveld structure refinement of data obtained by heating and cooling from 26 to 902°C. The structure was refined in space group $P4_2/n$. A room-temperature structure, obtained with synchrotron high-resolution powder X-ray-diffraction (HRPXRD) data, has unit-cell parameters a 12.06503(1), c 7.58360(1) Å, and V 1103.906(2) Å^3. Moreover, the average bond-distances $<T1–O>$, $<T2–O>$ and $<T3–O>$ are equal to 1.606(2), 1.726(2) and 1.612(2) Å, respectively, and correspond to occupancies $T1 = [Al_0Si_1]$, $T2 = [Al_{0.87}Si_{0.13}]$, and $T3 = [Al_{0.02}Si_{0.98}]$. At 902°C, $<T1–O>$, $<T2–O>$ and $<T3–O>$ are equal to 1.591(5), 1.683(8) and 1.686(7) Å, respectively, and correspond to $T1 = [Al_0Si_1]$, $T2 = [Al_{0.55}Si_{0.45}]$, and $T3 = [Al_{0.57}Si_{0.43}]$. At 902°C, the $T1$ site remains fully occupied by Si atoms, whereas the disorder at the $T2$ and $T3$ sites is close to being complete. Several structural parameters show a break at 200°C, which corresponds to disorder of the Na and Ca (= M) atoms. On cooling, the structure does not go back to the initial structural state; some $T2$–$T3$ and Na–Ca disorder are quenched in. The type-b reflections that give rise to antiphase-domain boundaries (APBs) are present at all temperatures; they arise from Cl–CO_3 order, instead of Al–Si order. At 902°C, except for the anions, there is no difference between the structure of $Me_{32.9}$ in space group $P4_2/n$ and that of Me_{80} in space group $I4/m$.

Keywords: scapolite group, marialite, high-temperature crystal structure, Al–Si and Na–Ca disorder, APBs, synchrotron X-ray diffraction.

SOMMAIRE

Nous avons étudié la composition $Me_{32.9}$ (marialite) du groupe de la scapolite provenant du canton de Monmouth, en Ontario, au moyen de diffraction X *in situ* sur poudre avec rayonnement synchrotron, et d'affinements de la structure par la méthode de Rietveld à partir de données prélevées en chauffant et en refroidissant l'échantillon entre 26° et 902°C. Nous avons affiné la structure dans le groupe spatial $P4_2/n$. La structure à température ambiante, obtenue par diffraction X à haute résolution avec rayonnement synchrotron (HRPXRD), a donné les paramètres réticulaires a 12.06503(1), c 7.58360(1) Å, et V 1103.906(2) Å^3. Les longueurs moyennes des liaisons $<T1–O>$, $<T2–O>$ et $<T3–O>$ sont égales à 1.606(2), 1.726(2) et 1.612(2) Å, respectivement, et correspondent aux distributions $T1 = [Al_0Si_1]$, $T2 = [Al_{0.87}Si_{0.13}]$, et $T3 = [Al_{0.02}Si_{0.98}]$. A 902°C, les distances $<T1–O>$, $<T2–O>$ et $<T3–O>$ sont égales à 1.591(5), 1.683(8) et 1.686(7) Å, respectivement, et correspondent à $T1 = [Al_0Si_1]$, $T2 = [Al_{0.55}Si_{0.45}]$, et $T3 = [Al_{0.57}Si_{0.43}]$. A 902°C, le site $T1$ demeure entièrement rempli d'atomes Si, tandis que le désordre aux sites $T2$ et $T3$ est presque complet. Plusieurs paramètres structuraux montrent une discontinuité à 200°C, ce qui correspond à l'inception de désordre impliquant les atomes Na et Ca (= M). En refroidissant, les atomes ne retournent pas à leurs distributions initiales; une partie du désordre impliquant $T2$–$T3$ et Na–Ca demeure. Les réflections de type b qui mènent au développement de parois de domaines anti-phasés (APB) sont présents à toutes températures; elles seraient dues à une mise en ordre de Cl et CO_3 plutôt que de Al et Si. A 902°C, sauf pour les anions, il n'y a aucune différence entre la structure de $Me_{32.9}$ dans le groupe spatial $P4_2/n$ et celle de Me_{80} dans le groupe spatial $I4/m$.

(Traduit par la Rédaction)

Mots-clés: groupe de la scapolite, marialite, structure cristalline à température élevée, désordre Al–Si et Na–Ca, APB, diffraction X avec rayonnement synchrotron.

§ Present address: Department of Geoscience, University of Calgary, Calgary, Alberta T2N 1N4, Canada.
E-mail address: antao@ucalgary.ca

Introduction

Scapolite, a group of framework aluminosilicate minerals, $(Na,Ca,K)_4[(Al,Si)_3Al_3Si_6O_{24}](Cl,CO_3,SO_4)$, occurs in a variety of rocks. It forms solid solutions among the end-members marialite, $Na_4[Al_3Si_9O_{24}]Cl$ (Me_0), meionite, $Ca_4[Al_6Si_6O_{24}]CO_3$ (Me_{100}), and $Ca_4[Al_6Si_6O_{24}]SO_4$ (silvialite) (Deer *et al.* 1992, Teertstra *et al.* 1999). The percentage of meionite [Me% = 100 Ca/(Na + Ca + K)] is used to indicate the composition of scapolite (Shaw 1960). The composition varies by replacement of $[Na_4{\bullet}Cl]Si_2$ for $[NaCa_3{\bullet}CO_3]Al_2$ from Me_0 to Me_{75} (series 1), whereas from Me_{75} to Me_{100} (series 2), it is governed by the replacement of $[NaCa_3{\bullet}CO_3]Si$ for $[Ca_4{\bullet}CO_3]Al$; SO_4 may replace CO_3 (Evans *et al.* 1969, Hassan & Buseck 1988). Based on results of electron microscopy, the cage clusters, $[Na_4{\bullet}Cl]^{3+}$ and $[NaCa_3{\bullet}CO_3]^{5+}$, are ordered in series 1, whereas $[NaCa_3{\bullet}CO_3]^{5+}$ and $[Ca_4{\bullet}CO_3]^{6+}$ are disordered in series 2 (Hassan & Buseck 1988).

Several studies (*e.g.*, Sokolova *et al.* 1996, 2000, Teertstra & Sherriff 1996, Sherriff *et al.* 1998, 2000, Seto *et al.* 2004), indicate a division of the scapolite series into three subseries. We maintain the division of the series into two that meet compositionally at Me_{75} (*e.g.*, Evans *et al.* 1969, Hassan & Buseck 1988, Deer *et al.* 1992). Moreover, across the Me_0–Me_{100} series, there are breaks in unit cell and several other structural parameters at Me_{75} (our unpublished data).

Composition $Me_{32.9}$ was chosen for this study because differential thermal analysis (DTA), thermogravimetry (TG), and differential scanning calorimetry (DSC) indicate disordering of the Na–Ca (= *M*) atoms from 200° to 400°C with a peak temperature at about 300°C (Antao & Hassan 2002). These scans indicate that scapolite $Me_{32.9}$ is stable within the *T* range of this study; loss of volatiles (CO_2, Cl) occurs at 1199°C, and melting occurs at 1319°C.

The type-*b* reflections ($h + k + l$ = odd), in particular the (021) reflection, are absent in space group $I4/m$, but are present in space group $P4_2/n$ and give rise to antiphase domain boundaries (APBs). The APBs are observed in electron microscopy by imaging using type-*b* reflections. With Al–Si disorder, the type-*b* reflections and APBs should be lost, if they are related. The type-*b* reflections and APBs should be present if Cl and CO_3 remain ordered at all temperatures, but the *M* cations can be disordered without effect on the space group or APBs. We test these possibilities in the present study.

In this study, we provide evidence that the APBs in scapolite arise from Cl–CO_3 order, and not from Al–Si order. Disorder of Al and Si occurs at the *T*2–*T*3 sites near 900°C, but no disorder occurs at the *T*1 site. The type-*b* reflections (and APBs) are present on heating to 902°C, the Cl–CO_3 anions remain ordered, and no change in space group occurs. The present results on $Me_{32.9}$ are compared to those of $Me_{79.6}$ (Antao & Hassan 2008a).

Background Information

The structure of intermediate scapolite, $M_4[T_{12}O_{24}]A$, $Z = 2$, space group $P4_2/n$, consists of AlO_4 and SiO_4 tetrahedra that form two types of four-membered rings. The type-1 ring consists of *T*1 tetrahedra that point in the same direction, whereas the type-2 ring consists of *T*2 and *T*3 tetrahedra that point alternately up and down (Fig. 1). Five-membered rings occur along columns parallel to the **c** axis (Fig. 2). Continuous oval channels contain mainly Na^+ and Ca^{2+} (with minor K^+) cations (the *M* site), and the cages contain Cl^-, CO_3^{2-}, and SO_4^{2-} anions (the *A* site). Each *A* anion is coordinated by four *M* cations (Fig. 2). On the basis of electron microscopy results (Hassan & Buseck 1988), the cage clusters, $[Na_4{\bullet}Cl]^{3+}$ and $[NaCa_3{\bullet}CO_3]^{5+}$, are ordered at the corners [P1 = (0, 0, 0)] and center [P2 = (½, ½, ½)] of the unit cell. The observed order in the cluster is supported by energy calculations on the structure (Chamberlain *et al.* 1985). Scapolite $Me_{32.9}$ contains APBs that arise from order of clusters, particularly, order of Cl and CO_3 anions (Phakey & Ghose 1972, Hassan & Buseck 1988); the occupancies of the P1 and P2 sites by these anions are switched at the domain boundaries. Because of cluster order and evidence from electron diffraction, the space group of intermediate scapolite is lower than $P4_2/n$ or $I4/m$ (see Phakey & Ghose 1972). Others have suggested that the observed APBs arise from Al–Si order, but no experimental

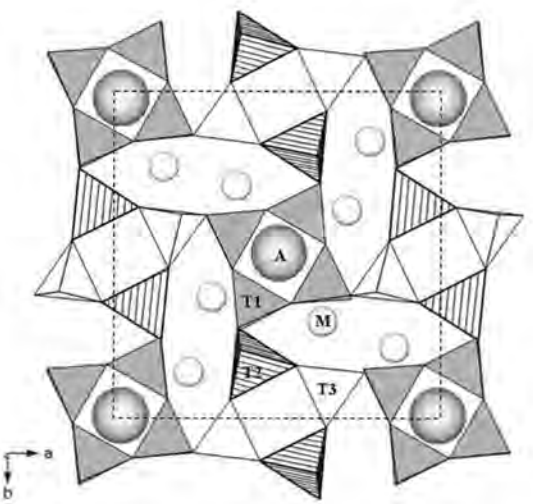

FIG. 1. Structure of $P4_2/n$ scapolite projected along the **c** axis and showing the *T*, *M*, and *A* sites, as well as the four-membered rings and oval channels. A unit cell is indicated.

evidence was given (Oterdoom & Wenk 1983, Seto *et al.* 2004).

The *M*–*A* (*e.g.*, Na–Cl) distance in scapolite is anomalously large [3.032(1) Å], compared to that in sodalite [2.730(1) Å; Hassan & Grundy 1984, Hassan *et al.* 2004], but no explanation is available for this observation (Levien & Papike 1976). A disorder of the *M* cations should produce Na–Cl distances closer to those observed in sodalite.

Experimental

Scapolite $Me_{32.9}$ is white and occurs in a coarsely crystalline sample of calcareous gneiss from Monmouth Township, Ontario, labeled ON7 (Evans *et al.* 1969). Sample ON7 is well characterized (*e.g.*, Evans *et al.* 1969, Hassan & Buseck 1988, Teertstra & Sherriff 1996, Antao & Hassan 2002). Crystals of this sample of marialite were hand-picked under a microscope, and finely ground in an agate mortar and pestle for the X-ray-diffraction experiments that were performed at the Advanced Photon Source (APS), Argonne National Laboratory.

The experimental procedures used in this study, including those at beamline 11–BM, were recently described for scapolite $Me_{79.6}$ (meionite) and are not repeated here (Antao & Hassan 2008a); in addition, the 11–BM set-up is also described elsewhere (Antao & Hassan 2008b, c, Antao *et al.* 2008). A room-temperature structure was obtained by Rietveld refinement based on synchrotron high-resolution powder X-ray-diffraction (HRPXRD) data from beamline 11–BM. The high-temperature synchrotron powder X-ray-diffraction (XRD) experiments were performed at beamline 1–BM and are based on image plate (IP) data. Typical diffraction traces are displayed (Figs. 3, 4).

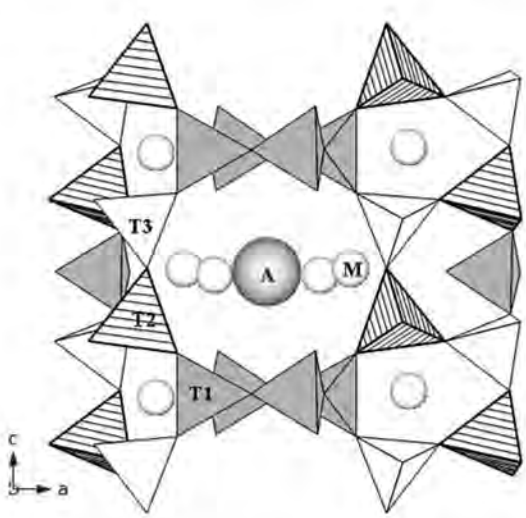

FIG. 2. Part of $P4_2/n$ scapolite structure showing a cage containing *M* cations and an *A* anion. A few five-membered rings are shown.

Rietveld Structure Refinement

The chemical formula for scapolite $Me_{32.9}$ is $(Ca_{1.29}Na_{2.36}K_{0.28})[Si_{8.08}Al_{3.92}O_{24}]Cl_{0.61}(CO_3)_{0.30}(SO_4)_{0.02}$ (Evans *et al.* 1969). The space group $P4_2/n$ and initial structural parameters were taken from Levien & Papike (1976). The structure was modeled using the Rietveld method (Rietveld 1969), as implemented in the GSAS program (Larson & Von Dreele 2000), and using the EXPGUI interface (Toby 2001). The structure refinement was carried out in the following sequence: refinement of a scale factor, background, cell, zero shift, profile, atom positions, and displacement parameters. Finally, all variables were refined simultaneously.

The HRPXRD data at room temperature was refined using anisotropic displacement parameters. We assume that the *M* site is fully occupied by Na and Ca atoms, and their site-occupancy factors (*sof*) were refined. We also assume that the *A* site is fully occupied by Cl and C atoms, and their *sof* were refined. The *sof* for the O7C atom belonging to the CO_3 group was constrained to equal the C *sof*. The O7C atom was refined isotropically.

The HRPXRD structural model (and *sof* for the *M* and *A* sites) was then used for refinement of the IP data at room temperature, and the results were then used as input for the next higher-temperature structure. For the IP data, the *sof* for each site was considered invariant and fixed to the *sof* obtained from the HRPXRD data. All atoms were refined using isotropic displacement parameters.

Cell parameters and refinement statistics are given in Table 1. Positional coordinates and displacement parameters are given in Table 2. Table 3 contains the anisotropic displacement parameters obtained from the HRPXRD data. Bond distances and angles are given in Table 4. These tables contain information for only a few selected temperatures, but all results are displayed graphically.

Results and Discussion

Room-temperature structure

The room-temperature structural parameters for $Me_{32.9}$ from the two datasets are similar to each other, but those obtained by HRPXRD provide better parameters than the IP data because of the superior experimental set-up (sharp peaks, high resolution, and larger 2θ range). The number of observed reflections was 1590 from HRPXRD compared to 320 from IP data. The close similarity between the two structures at room temperature gives us confidence that detailed structural parameters can be obtained at high temperature using

our present IP data. Our room-temperature structure is similar to that of $Me_{35.1}$ (Levien & Papike 1976).

The $Me_{32.9}$ cell parameters obtained from HRPXRD data are a 12.06503(1), c 7.58360(1) Å, and V 1103.906(2) Å^3. The average values of <$T1$–O>, <$T2$–O> and <$T3$–O>, 1.606(2), 1.726(2) and 1.612(2) Å, respectively, correspond to occupancies of $T1 = [Al_0Si_1]$, $T2 = [Al_{0.87}Si_{0.13}]$, and $T3 = [Al_{0.02}Si_{0.98}]$ based on Si–O = 1.6100(2) Å and Al–O = 1.7435(2) Å, as observed in sodalite, $Na_8[Al_6Si_6O_{24}]Cl_2$ (Antao & Hassan 2008c). The $T1$ site contains only Si atoms, whereas the $T2$ and $T3$ sites are almost fully ordered at room temperature. Our refined *sof* values for the M and A sites are similar to those obtained from the chemical analysis. The *sof* for Ca is 0.305(4) (and Na = 1 – 0.305) and gives rise to $Me_{30.5}$ compared to $Me_{32.9}$ obtained by chemical analysis (Evans *et al.* 1969). The *sof* for Cl is 0.759(6) (and C = 1 – 0.759).

Unit-cell parameters

The variation of the cell parameters with temperature is shown (Fig. 5). The room-temperature cell parameters match closely in the two datasets. On heating to 902°C, the a parameter and volume increase smoothly and nonlinearly, whereas the c parameter decreases steeply to about 200°C, indicating a negative thermal-expansion behavior. The ratio c/a decreases with increasing temperature. On cooling from 902° to 36°C, the a, c/a, and V parameters reverse on a slightly different path (Fig. 5). The trends on heating and cooling for the c parameter are different, and there is a break between 192 and 251°C (Fig. 5b). Scapolite $Me_{79.6}$ was found to show similar features for the a, c/a, and V parameters, but its c parameter was found to increase with temperature, and on cooling it was found to decrease significantly (Antao & Hassan 2008a). Where the cell parameters are plotted as the d/d_0 ratio, one can see that the **a** axis expands much more than the **c** axis (Fig. 6). There appears to be a break in the a and V parameters at about 516°C (Figs. 5, 6). These results contrast with previous studies, where linear increases were reported for a and V, whereas c was found to be nearly constant (Levien & Papike 1976, Graziani & Lucchesi 1982, Baker 1994). However, a decrease in c was reported for marialite (Kabalov *et al.* 1999).

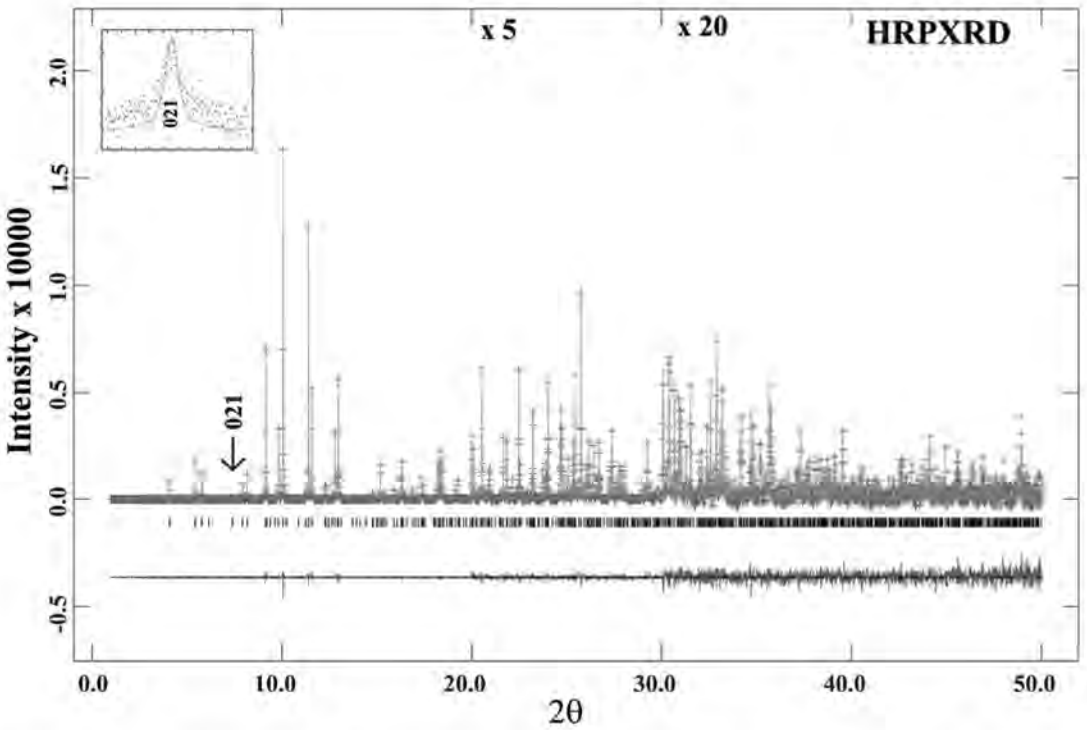

FIG. 3. HRPXRD trace for scapolite $Me_{32.9}$ at room temperature, together with the calculated (continuous line) and observed (crosses) profiles. The difference curve ($I_{obs} - I_{calc}$) is shown at the bottom. The short vertical lines indicate allowed reflection positions. Note that the intensities beyond 20 and 30° are scaled differently. The (021) reflection is pointed out and also shown as an insert.

<T–O> distances and T–O–T angles

We report variations of the bond distances with temperature in Figure 7. The average <*T*1–O> distance decreases slightly to 902°C because of thermal motion (Fig. 7a). The <*T*2–O> and <*T*3–O> distances show opposite effects, and changes occur at about 200 and 889°C on heating, and between 251 and 312°C on cooling (Fig. 7b). The average for both <*T*2,*T*3–O> is nearly constant to 889°C (Fig. 7a). Apart from minor variations below about 100°C, which probably arise from structural strain because of order of two different sizes of anions (Cl *versus* CO_3), the <*T*2–O> and <*T*3–O> distances are nearly constant up to 889°C; thereafter, <*T*2–O> decreases, whereas <*T*3–O> increases, and they are nearly equal at 902°C within experimental error [<*T*2–O> = 1.683(8) Å and <*T*3–O> = 1.686(7) Å]. Therefore, at 902°C, the *T*2–*T*3 sites are fully disordered on the basis of <*T*–O> distance and deduced *T*-site occupancy. The <*T*–O> distances do not revert to the initial values on cooling; some quenching of the high-T disordered state occurs. In scapolite $Me_{79.6}$, Al–Si disorder occurs at about 900°C, and no change occurs at 200°C (Antao & Hassan 2008a).

The *T*2 site in scapolite $Me_{79.6}$ becomes more Al-rich from 892 to 900°C (it changes from $[Al_{0.45}Si_{0.55}]$ to $[Al_{0.51}Si_{0.49}]$), whereas the *T*1 site becomes more Si rich (it changes from $[Al_{0.11}Si_{0.89}]$ to $[Al_0Si_1]$, such that full order of the *T*1 site occurs at 900°C). This is an unusual behavior for the *T*1 site, as atoms are expected to disorder with increasing temperature. In scapolite $Me_{32.9}$, the *T*1 site contains Si atoms at all temperatures. Small amounts of Al–Si disorder and changes in cell parameters (before and after heating) were reported for scapolite $Me_{35.1}$ (Levien & Papike 1976).

Changes occur in the *T*–O–*T* bridging angles near 900°C (Fig. 8). The trends on cooling are different, with only the average <*T*–O–*T*> angle reverting back to the initial value at room temperature (Fig. 8a). On heating, changes at about 200°C are minor for the *T*2–O3–*T*3 and *T*2–O4–*T*3 angles (Fig. 8c), whereas they are more significant for the *T*1–O5–*T*2 and *T*1–O6–*T*3 angles (Fig. 8b). On cooling, changes occur between 251° and 312°C (Fig. 8b).

<M–O> and <M–A> distances, and Na–Ca disorder

The <*M*–O> distances increase with temperature (Fig. 9a). The <*M*–O>[7] variation is more uniform than <*M*–O>[9], which includes two distances to O7C atoms belonging to the positionally disordered CO_3 group. The <*M*–O> distance varies continuously and smoothly on cooling to room temperature.

The *M*–*A* distance is one of the most accurately determined because the *A* site is fixed and the *M* position is well defined. On heating, the *M*–*A* distance remains constant, then increases at 200°C (arrow in Fig. 9b), decreases with temperature, and increases significantly near 900°C. On cooling, the *M*–*A* distance is almost constant to 251°C, and then increases to room temperature. The *M*–*A* distance contains the effects of *M* cation disorder (the *A* site contains Cl and C atoms). For $Me_{79.6}$, with no cluster order, the *M*–*A* distance increases smoothly to 900°C (Antao & Hassan 2008a). For $Me_{32.9}$, the break in the *M*–*A* distance at 200°C indicates *M* cation disorder. This feature was observed from 200 to 400°C with a peak *T* at about 300°C in thermal analyses (Antao & Hassan 2002). The break at 200°C that arises from Na–Ca disorder was observed in several structural parameters, including the **c** axis (Fig. 5b), C–O7C distance (Fig. 9c) and, particularly, the *z* coordinate of the *M* site (Fig. 9d). The whole structure re-adjusts at 200°C. On cooling, the *z* coordinate changes between 251° and 312°C, where changes are also observed along the **c** axis. The disorder of the Na–Ca cations may be considered as a transition at 200°C, possibly of second order.

At room temperature, the *M*–*A* distance is 3.032(1) Å, which is quite large for a Na–Cl bond (and way too large for a Ca–Cl bond), compared to 2.730(1) Å in sodalite (Hassan & Grundy 1984). Disorder of the *M* cations causes the *M*–*A* distance to become shorter in an attempt to form a more realistic distance. At 700°C, the *M*–*A* distance is about 3 Å (Fig. 9b), whereas it is 2.832(3) Å at about the same temperature in sodalite (Hassan *et al.* 2004). The scapolite structure

TABLE 1. UNIT-CELL AND RIETVELD REFINEMENT STATISTICS FOR SCAPOLITE $Me_{32.9}$ (MARIALITE) AT SELECTED TEMPERATURES

T °C	*a* (Å)	*c* (Å)	*V* (Å³)	R_F^2 *
		HRPXRD data		
25	12.06503(1)	7.58360(1)	1103.906(2)	0.0636
		Heating (IP data)		
26	12.0652(2)	7.5827(2)	1103.79(4)	0.0337
105	12.0749(2)	7.5814(2)	1105.39(4)	0.0336
204	12.0882(2)	7.5808(2)	1107.74(4)	0.0327
305	12.1025(2)	7.5804(2)	1110.30(4)	0.0345
405	12.1172(2)	7.5800(2)	1112.94(4)	0.0365
505	12.1335(2)	7.5801(2)	1115.96(4)	0.0404
603	12.1510(2)	7.5800(2)	1119.17(4)	0.0428
702	12.1673(3)	7.5799(2)	1122.16(4)	0.0447
801	12.1844(2)	7.5799(2)	1125.30(4)	0.0439
902	12.1974(3)	7.5795(2)	1127.65(6)	0.0655
		Cooling (IP data)		
870	12.1921(4)	7.5796(3)	1126.68(7)	0.0771
814	12.1823(4)	7.5798(3)	1124.91(7)	0.0795
751	12.1724(4)	7.5802(3)	1123.15(7)	0.0784
690	12.1626(4)	7.5806(3)	1121.39(6)	0.0815
625	12.1514(4)	7.5802(3)	1119.27(6)	0.0795
561	12.1412(4)	7.5797(3)	1117.30(6)	0.0734
499	12.1316(4)	7.5794(3)	1115.49(6)	0.0707
437	12.1219(4)	7.5791(3)	1113.67(6)	0.0740
373	12.1127(4)	7.5789(3)	1111.95(6)	0.0706
312	12.1038(4)	7.5787(3)	1110.30(6)	0.0635
251	12.0952(4)	7.5787(3)	1108.72(6)	0.0611
192	12.0856(4)	7.5773(3)	1106.76(6)	0.0575
133	12.0770(4)	7.5768(3)	1105.11(7)	0.0569
36	12.0645(4)	7.5765(3)	1102.77(6)	0.0540

* R_F^2 = R structure-factor based on observed and calculated structure-amplitudes = $[\Sigma(F_o^2 - F_c^2)^2 / \Sigma(F_o^2)^2]^{1/2}$.

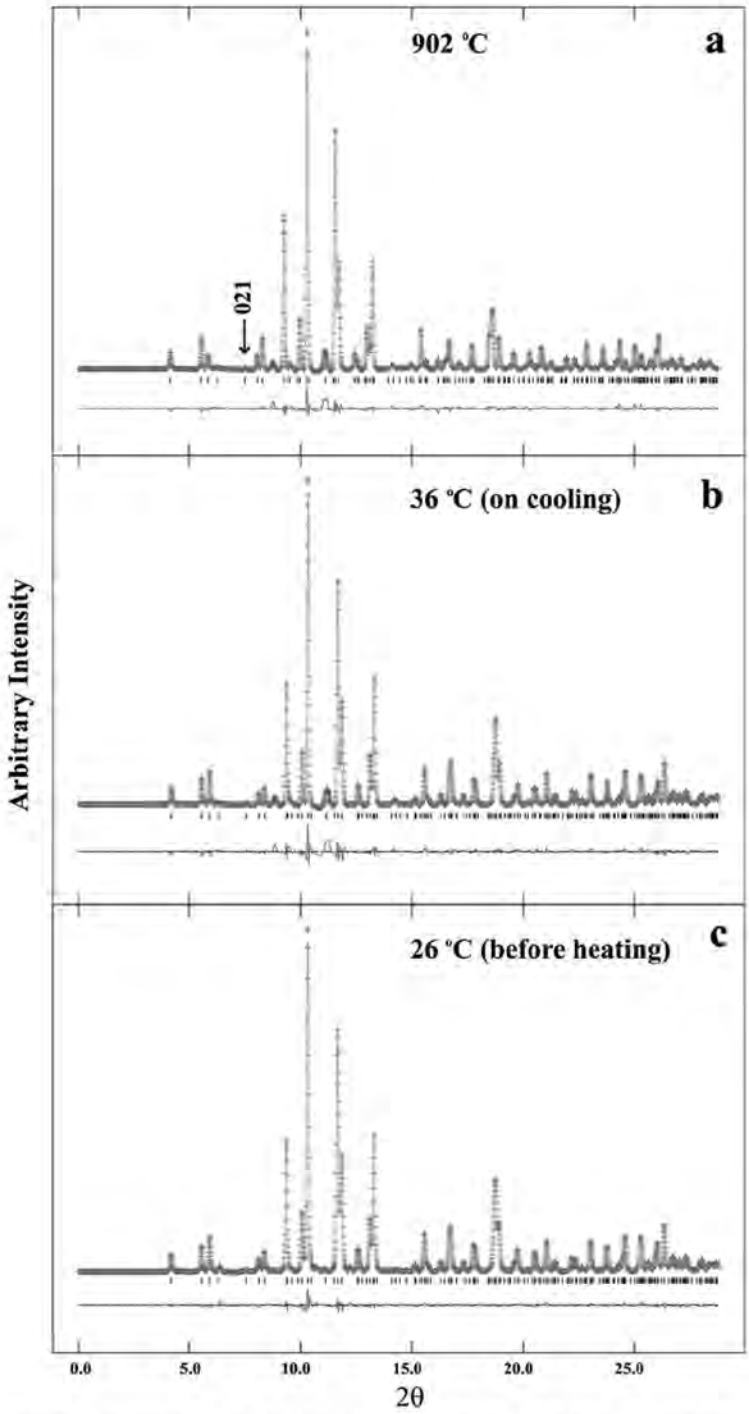

FIG. 4. Comparison of the XRD traces for scapolite $Me_{32.9}$ at (a) 902°C, (b) 36°C on cooling, and (c) 26°C before heating, together with the calculated (continuous line) and observed (crosses) profiles. The difference curve ($I_{obs} - I_{calc}$) is shown at the bottom. The short vertical lines indicate allowed reflection positions. The (021) reflection is observed at all temperatures (arrow).

TABLE 2. ATOM POSITIONS AND ISOTROPIC DISPLACEMENT PARAMETERS AT SELECTED *T* FOR SCAPOLITE $Me_{32.9}$ (MARIALITE)

T°C		25 (HRPXRD)*	26	105	204	305	405	505	603	702	801	902
*T*1	*x*	0.5896(1)	0.5905(3)	0.5898(3)	0.5889(3)	0.5883(3)	0.5881(3)	0.5882(3)	0.5880(3)	0.5876(3)	0.5874(3)	0.5904(4)
	y	0.6594(1)	0.6608(3)	0.6612(2)	0.6613(2)	0.6615(2)	0.6616(3)	0.6620(3)	0.6623(3)	0.6624(3)	0.6633(3)	0.6646(4)
	z	0.2472(3)	0.2609(13)	0.2545(18)	0.2481(14)	0.2452(13)	0.2428(14)	0.2427(13)	0.2447(16)	0.2498(20)	0.2547(18)	0.2539(16)
	U†	0.0078	0.0191(9)	0.0180(4)	0.0174(8)	0.0186(8)	0.0198(8)	0.0219(8)	0.0247(9)	0.0267(10)	0.0291(10)	0.0322(9)
*T*2	*x*	0.9103(2)	0.9076(6)	0.9093(5)	0.9095(6)	0.9096(6)	0.9095(6)	0.9098(6)	0.9101(6)	0.9105(7)	0.9110(7)	0.9111(6)
	y	0.1653(2)	0.1677(7)	0.1675(6)	0.1677(6)	0.1678(6)	0.1677(6)	0.1676(6)	0.1678(7)	0.1681(7)	0.1690(7)	0.1699(8)
	z	0.0482(2)	0.0494(9)	0.0506(9)	0.0484(11)	0.0501(10)	0.0534(10)	0.0541(9)	0.0549(10)	0.0556(10)	0.0551(9)	0.0574(9)
*T*3	*x*	0.6636(2)	0.6644(7)	0.6657(7)	0.6661(6)	0.6666(6)	0.6670(6)	0.6677(6)	0.6685(7)	0.6690(7)	0.6696(7)	0.6700(8)
	y	0.0857(2)	0.0861(6)	0.0874(5)	0.0869(6)	0.0872(6)	0.0873(6)	0.0871(6)	0.0874(6)	0.0882(7)	0.0886(7)	0.0859(7)
	z	0.9600(2)	0.9605(10)	0.9622(8)	0.9602(11)	0.9610(10)	0.9627(9)	0.9625(9)	0.9620(9)	0.9617(9)	0.9603(8)	0.9626(10)
M	*x*	0.6158(1)	0.6162(2)	0.6163(2)	0.6164(2)	0.6170(3)	0.6174(3)	0.6176(3)	0.6177(3)	0.6178(3)	0.6176(3)	0.6153(4)
	y	0.5377(1)	0.5383(3)	0.5385(3)	0.5386(3)	0.5394(3)	0.5403(3)	0.5410(3)	0.5417(4)	0.5425(4)	0.5426(4)	0.5409(6)
	z	0.7616(3)	0.7542(13)	0.7569(12)	0.7429(13)	0.7435(13)	0.7502(19)	0.7538(17)	0.7549(19)	0.7548(20)	0.7557(18)	0.7477(20)
	U	0.0306	0.040(1)	0.042(1)	0.046(1)	0.052(1)	0.058(1)	0.062(1)	0.070(2)	0.077(2)	0.084(2)	0.082(2)
O1	*x*	0.7081(2)	0.7090(5)	0.7093(4)	0.7091(4)	0.7091(4)	0.7091(5)	0.7092(5)	0.7091(5)	0.7088(5)	0.7079(5)	0.7056(8)
	y	0.6015(2)	0.6021(4)	0.6029(4)	0.6038(4)	0.6048(4)	0.6058(4)	0.6061(4)	0.6068(5)	0.6080(5)	0.6081(4)	0.6005(7)
	z	0.2507(4)	0.2535(21)	0.2533(19)	0.2596(21)	0.2602(21)	0.2529(26)	0.2449(27)	0.2429(26)	0.2454(26)	0.2478(24)	0.2479(32)
	U	0.015	0.028(1)	0.027(1)	0.026(1)	0.026(1)	0.029(1)	0.033(1)	0.037(1)	0.040(1)	0.044(1)	0.046(2)
O2	*x*	0.9430(2)	0.9450(4)	0.9448(4)	0.9444(4)	0.9443(4)	0.9443(4)	0.9441(4)	0.9443(5)	0.9440(5)	0.9444(5)	0.9525(6)
	y	0.1281(2)	0.1281(4)	0.1293(4)	0.1308(4)	0.1319(4)	0.1326(4)	0.1333(4)	0.1343(4)	0.1354(4)	0.1365(4)	0.1340(6)
	z	0.2639(4)	0.2582(22)	0.2702(16)	0.2741(15)	0.2734(15)	0.2715(15)	0.2715(14)	0.2725(16)	0.2724(16)	0.2695(17)	0.2622(26)
O3	*x*	0.6003(3)	0.5949(9)	0.5935(7)	0.5939(9)	0.5940(9)	0.5933(8)	0.5924(8)	0.5927(8)	0.5930(9)	0.5938(8)	0.5969(10)
	y	0.1931(3)	0.1896(8)	0.1870(8)	0.1860(8)	0.1857(7)	0.1861(8)	0.1870(8)	0.1876(9)	0.1875(9)	0.1868(8)	0.1945(10)
	z	0.0419(4)	0.0348(17)	0.0360(15)	0.0359(19)	0.0333(18)	0.0302(19)	0.0295(18)	0.0288(19)	0.0274(21)	0.0258(20)	0.0285(23)
O4	*x*	0.7953(2)	0.7992(9)	0.7973(8)	0.7961(9)	0.7957(9)	0.7957(9)	0.7966(9)	0.7969(10)	0.7971(10)	0.7978(10)	0.8059(10)
	y	0.0990(3)	0.1010(9)	0.1033(8)	0.1042(9)	0.1044(8)	0.1052(8)	0.1064(8)	0.1070(8)	0.1065(9)	0.1068(8)	0.1152(11)
	z	0.9667(4)	0.9672(15)	0.9689(13)	0.9705(16)	0.9710(15)	0.9702(16)	0.9705(16)	0.9725(18)	0.9740(20)	0.9744(18)	0.9772(24)
O5	*x*	0.5192(2)	0.5121(9)	0.5162(9)	0.5171(9)	0.5167(9)	0.5152(9)	0.5143(9)	0.5146(10)	0.5154(11)	0.5186(11)	0.5055(10)
	y	0.6204(3)	0.6155(6)	0.6162(7)	0.6155(7)	0.6153(6)	0.6162(7)	0.6181(7)	0.6196(8)	0.6202(9)	0.6217(8)	0.6221(8)
	z	0.0820(4)	0.0900(13)	0.0877(13)	0.0719(13)	0.0725(13)	0.0776(18)	0.0794(17)	0.0806(19)	0.0841(20)	0.0866(19)	0.1080(15)
O6	*x*	0.6228(3)	0.6281(7)	0.6291(7)	0.6314(7)	0.6329(7)	0.6341(8)	0.6338(8)	0.6341(9)	0.6348(10)	0.6361(10)	0.6381(9)
	y	0.9782(2)	0.9729(8)	0.9756(9)	0.9754(9)	0.9754(9)	0.9747(9)	0.9744(9)	0.9751(10)	0.9772(11)	0.9802(11)	0.9637(9)
	z	0.0743(4)	0.0616(12)	0.0639(12)	0.0791(13)	0.0798(13)	0.0771(17)	0.0772(16)	0.0770(18)	0.0758(19)	0.0750(18)	0.0638(15)
O7C	*x*	0.7645(14)	0.7702(52)	0.7899(40)	0.8061(33)	0.8192(32)	0.8265(33)	0.8266(33)	0.8294(38)	0.8407(45)	0.8407(43)	0.7758(115)
	y	0.6405(9)	0.6480(26)	0.6507(25)	0.6545(29)	0.6644(35)	0.6703(39)	0.6703(39)	0.6726(44)	0.6896(57)	0.6904(55)	0.6539(48)
	z	0.7387(32)	0.754(18)	0.748(16)	0.748(16)	0.746(16)	0.749(19)	0.749(21)	0.749(23)	0.753(24)	0.752(21)	0.8305(76)
	U	0.048(6)	0.093(4)	0.090(4)	0.087(4)	0.096(4)	0.103(4)	0.108(4)	0.117(5)	0.130(5)	0.141(5)	0.162(7)

A is at (¾,¾,¾) and contains Cl and C atoms. * For HRPXRD data, values of *U* (in Å^2) are given in Table 3, except *U* (O7C), which was refined isotropically. In addition, *sof* values for Ca and Cl are 0.305(4) and 0.759(6), respectively, so the *sof* values for Na and C can be deduced. † For the IP data, the following constraints were used: T(1–3) have same *U*, O(1–6) have same *U*, and *U* (O7C) = *U* (A).

TABLE 3. ANISOTROPIC DISPLACEMENT PARAMETERS FROM HRPXRD DATA FOR SCAPOLITE $Me_{32.9}$ (MARIALITE)

Atom	$U_{eq.}$	U_{11}	U_{22}	U_{33}	U_{12}	U_{13}	U_{23}
*T*1	0.0078	0.0077(5)	0.0063(5)	0.0095(5)	-0.0008(5)	0.0001(12)	-0.0012(11)
*T*2	0.0083	0.0083(12)	0.0078(13)	0.0087(10)	-0.0024(10)	-0.0017(9)	0.0058(9)
*T*3	0.0105	0.0151(13)	0.0105(11)	0.0059(8)	-0.0005(9)	0.0014(9)	0.0031(9)
M	0.0306	0.0243(8)	0.0258(8)	0.0417(11)	0.0163(5)	0.0042(14)	-0.0013(14)
A	0.0664	0.0754(16)	0.0754(16)	0.0484(20)	0	0	0
O1	0.0150	0.0164(14)	0.0164(15)	0.0121(13)	0.0014(12)	0.0036(26)	0.0153(26)
O2	0.0203	0.0298(18)	0.0209(15)	0.0101(15)	0.0085(12)	-0.0032(24)	0.0184(21)
O3	0.0263	0.0344(37)	0.0180(25)	0.0265(26)	-0.0172(24)	0.0032(20)	-0.0080(18)
O4	0.0219	0.0365(29)	0.0208(32)	0.0084(22)	-0.0151(24)	-0.0051(18)	0.0015(18)
O5	0.0128	0.0220(27)	0.0072(24)	0.0091(21)	0.0037(22)	-0.0320(18)	0.0003(19)
O6	0.0237	0.0022(25)	0.0361(29)	0.0326(27)	-0.0039(21)	0.0016(20)	-0.0250(20)

TABLE 4. INTERATOMIC DISTANCES (Å) AND ANGLES (°) AT SELECTED T FOR SCAPOLITE $Me_{32.9}$ (MARIALITE)

T/°C	25 (HRPXRD)	26	105	204	305	405	505	603	702	801	902
*T*1-O1	1.592(2)	1.596(5)	1.606(5)	1.612(5)	1.619(5)	1.617(5)	1.617(5)	1.619(6)	1.616(6)	1.616(5)	1.607(8)
*T*1-O1'	1.604(2)	1.582(5)	1.573(5)	1.579(5)	1.579(5)	1.582(5)	1.581(5)	1.582(6)	1.587(6)	1.590(6)	1.589(8)
*T*1-O5	1.585(3)	1.694(12)	1.638(13)	1.686(11)	1.667(11)	1.628(14)	1.618(13)	1.616(14)	1.616(18)	1.607(18)	1.601(12)
*T*1-O6	1.643(4)	1.598(12)	1.634(14)	1.566(12)	1.572(12)	1.598(15)	1.599(13)	1.590(15)	1.575(18)	1.566(18)	1.566(13)
<*T*1-O>	**1.606(2)**	**1.618(5)**	**1.613(5)**	**1.611(4)**	**1.609(4)**	**1.606(5)**	**1.604(5)**	**1.602(6)**	**1.599(7)**	**1.595(7)**	**1.591(5)**
*T*2-O2	1.741(3)	1.714(15)	1.780(13)	1.818(13)	1.798(13)	1.758(14)	1.750(13)	1.749(15)	1.739(15)	1.721(14)	1.691(18)
*T*2-O3	1.715(3)	1.725(13)	1.760(12)	1.772(11)	1.778(11)	1.780(11)	1.774(11)	1.769(12)	1.770(13)	1.772(12)	1.671(16)
*T*2-O4	1.716(4)	1.658(11)	1.678(11)	1.678(11)	1.688(11)	1.696(11)	1.685(11)	1.681(12)	1.688(13)	1.689(12)	1.569(14)
*T*2-O5	1.730(3)	1.762(10)	1.775(10)	1.710(10)	1.717(11)	1.737(12)	1.730(12)	1.735(13)	1.758(14)	1.791(13)	1.800(12)
<*T*2-O>	**1.726(2)**	**1.715(6)**	**1.748(6)**	**1.745(6)**	**1.745(6)**	**1.743(6)**	**1.735(6)**	**1.734(7)**	**1.739(7)**	**1.743(6)**	**1.683(8)**
*T*3-O2	1.586(4)	1.639(16)	1.569(13)	1.522(13)	1.531(14)	1.556(15)	1.554(13)	1.544(15)	1.543(15)	1.555(14)	1.649(18)
*T*3-O3	1.627(4)	1.606(11)	1.587(10)	1.590(11)	1.579(10)	1.579(11)	1.600(11)	1.608(12)	1.601(13)	1.591(12)	1.674(14)
*T*3-O4	1.599(3)	1.636(13)	1.601(12)	1.587(12)	1.579(12)	1.576(11)	1.583(11)	1.581(12)	1.578(13)	1.581(13)	1.699(15)
*T*3-O6	1.636(4)	1.627(10)	1.616(10)	1.675(11)	1.676(11)	1.665(12)	1.672(11)	1.673(12)	1.657(13)	1.634(12)	1.720(11)
<*T*3-O>	**1.612(2)**	**1.627(6)**	**1.593(6)**	**1.594(6)**	**1.591(6)**	**1.594(6)**	**1.602(6)**	**1.602(6)**	**1.595(7)**	**1.590(6)**	**1.686(7)**
M-O2	2.361(3)	2.335(5)	2.353(5)	2.362(6)	2.374(6)	2.383(6)	2.392(6)	2.399(6)	2.406(7)	2.408(6)	2.289(8)
M-O3	2.533(4)	2.477(14)	2.465(13)	2.395(13)	2.416(13)	2.468(15)	2.494(14)	2.515(15)	2.532(17)	2.551(17)	2.553(20)
M-O4	2.507(4)	2.545(13)	2.569(11)	2.660(13)	2.668(13)	2.646(15)	2.642(14)	2.657(15)	2.669(17)	2.669(15)	2.752(22)
M-O5	2.874(4)	2.988(13)	2.937(13)	2.919(11)	2.922(11)	2.922(13)	2.922(15)	2.926(17)	2.945(17)	2.945(15)	3.199(16)
M-O5'	2.774(3)	2.691(9)	2.727(9)	2.837(11)	2.841(11)	2.808(13)	2.808(11)	2.824(12)	2.835(13)	2.862(12)	2.706(12)
M-O6	2.919(3)	3.025(9)	3.021(8)	2.945(10)	2.971(11)	3.029(13)	3.051(11)	3.063(12)	3.070(13)	3.069(12)	3.183(12)
M-O6'	2.971(4)	2.839(12)	2.889(12)	2.906(11)	2.921(11)	2.948(13)	2.969(14)	2.977(16)	2.979(16)	3.001(14)	2.812(16)
<*M*-O>[7]	**2.661(1)**	**2.677(4)**	**2.679(4)**	**2.686(4)**	**2.699(4)**	**2.709(5)**	**2.718(5)**	**2.731(5)**	**2.743(6)**	**2.751(5)**	**2.780(6)**
M-O7C	2.188(16)	2.28(6)	2.50(5)	2.69(5)	2.88(5)	2.98(5)	2.98(5)	3.02(6)	3.25(8)	3.26(8)	2.47(13)
M-O7C'	2.406(16)	2.34(6)	2.11(4)	1.93(4)	1.806(32)	1.737(30)	1.730(30)	1.70(4)	1.665(33)	1.678(31)	2.36(13)
<*M*-O>[9]	**2.615(3)**	**2.613(10)**	**2.619(8)**	**2.627(8)**	**2.644(7)**	**2.658(8)**	**2.665(7)**	**2.676(9)**	**2.706(11)**	**2.716(10)**	**2.703(21)**
M-*A*	3.032(1)	3.022(4)	3.022(3)	3.023(4)	3.015(4)	3.006(4)	3.003(4)	2.999(5)	2.994(5)	2.999(4)	3.033(7)
C-O7C × 4	1.336(12)	1.255(29)	1.292(25)	1.339(27)	1.333(28)	1.338(28)	1.341(27)	1.347(34)	1.326(31)	1.322(29)	1.36(5)
*T*1-O1-*T*1	159.1(2)	158.7(5)	159.7(4)	160.3(5)	161.3(6)	163.0(5)	162.9(6)	163.3(6)	164.6(6)	164.5(5)	155.3(7)
*T*2-O2-*T*3	139.6(1)	136.9(3)	137.3(3)	138.2(3)	138.6(3)	138.8(3)	139.1(3)	139.1(4)	139.4(4)	139.2(4)	133.8(5)
*T*2-O3-*T*3	147.1(2)	143.8(8)	142.1(8)	141.7(8)	142.3(7)	142.9(7)	142.7(7)	142.9(8)	143.2(8)	143.5(8)	148.6(9)
*T*2-O4-*T*3	149.5(3)	148.1(8)	150.1(8)	152.4(8)	152.3(8)	151.7(8)	152.3(9)	153.2(9)	153.2(10)	153.4(9)	155.8(12)
*T*1-O5-*T*2	139.9(2)	138.0(6)	137.3(6)	133.9(6)	133.9(6)	135.9(6)	137.7(7)	138.7(8)	139.2(8)	139.1(8)	142.2(7)
*T*1-O6-*T*3	138.7(2)	137.1(7)	137.8(7)	142.4(7)	142.7(7)	141.7(8)	141.3(8)	141.4(9)	142.4(10)	144.2(10)	135.5(7)
<*T*-O-T>	**145.6(1)**	**143.8(3)**	**144.1(3)**	**144.8(3)**	**145.2(3)**	**145.7(3)**	**146.0(3)**	**146.4(3)**	**147.0(3)**	**147.3(3)**	**145.2(3)**

is under severe strain at room temperature because of these unusual bond-distances, and the $[Na_4{\bullet}Cl]^{3+}$ and $[NaCa_3{\bullet}CO_3]^{5+}$ clusters order. Not much heating is required to release this strain, cause the *M* cations to disorder, and give rise to the transition at 200°C. Consequently, the **c** axis changes significantly before 200°C.

Antiphase domain boundaries (APBs)

The type-*b* reflections ($h + k + l$ = odd), in particular the (021) reflection, are absent in space group $I4/m$, whereas they are present in space group $P4_2/n$ and give rise to APBs (Phakey & Ghose 1972, Oterdoom & Wenk 1983, Seto *et al.* 2004). The (021) reflection was observed in the XRD traces at all temperatures in $Me_{32.9}$ (Fig. 4, arrow). Complete disorder of the *T*2–*T*3 sites makes them equivalent (= *T*2'), and the resulting structure of the framework is the same as the $I4/m$ structure of $Me_{79.6}$ (excluding the anions); both structures have only Si atoms at the *T*1 sites at 900°C. The structural relation may be seen by comparing the two samples. For $Me_{32.9}$ at 902°C, <*T*1–O> = 1.591(5) Å, <*T*2–O> = 1.683(8) Å, and <*T*3–O> = 1.686(7) Å, and they correspond to *T*1 = $[Al_0Si_1]$, *T*2 = $[Al_{0.55}Si_{0.45}]$, and *T*3 = $[Al_{0.57}Si_{0.43}]$. Therefore, at 902°C, the *T*1 site contains only Si atoms, whereas the *T*2 and *T*3 sites are close to complete disorder (*T*–O = 1.674 Å) within experimental error. For $Me_{79.6}$ at 900°C, <*T*1–O> = 1.609(3) Å, <*T*2–O> = 1.678(2) Å, and they correspond to *T*1 = $[Al_0Si_1]$ and *T*2 = $[Al_{0.51}Si_{0.49}]$. Therefore, the type-*b* reflections in $Me_{32.9}$ (and APBs) observed at all temperatures are not related to Al–Si order; they arise from Cl–CO_3 order. The Cl and CO_3 anions are ordered in each domain at all temperatures. Furthermore, if the APBs were to be caused by Al–Si order, the <*T*–O> distances would be expected to show wide fluctuations because different domain sizes would be averaged with

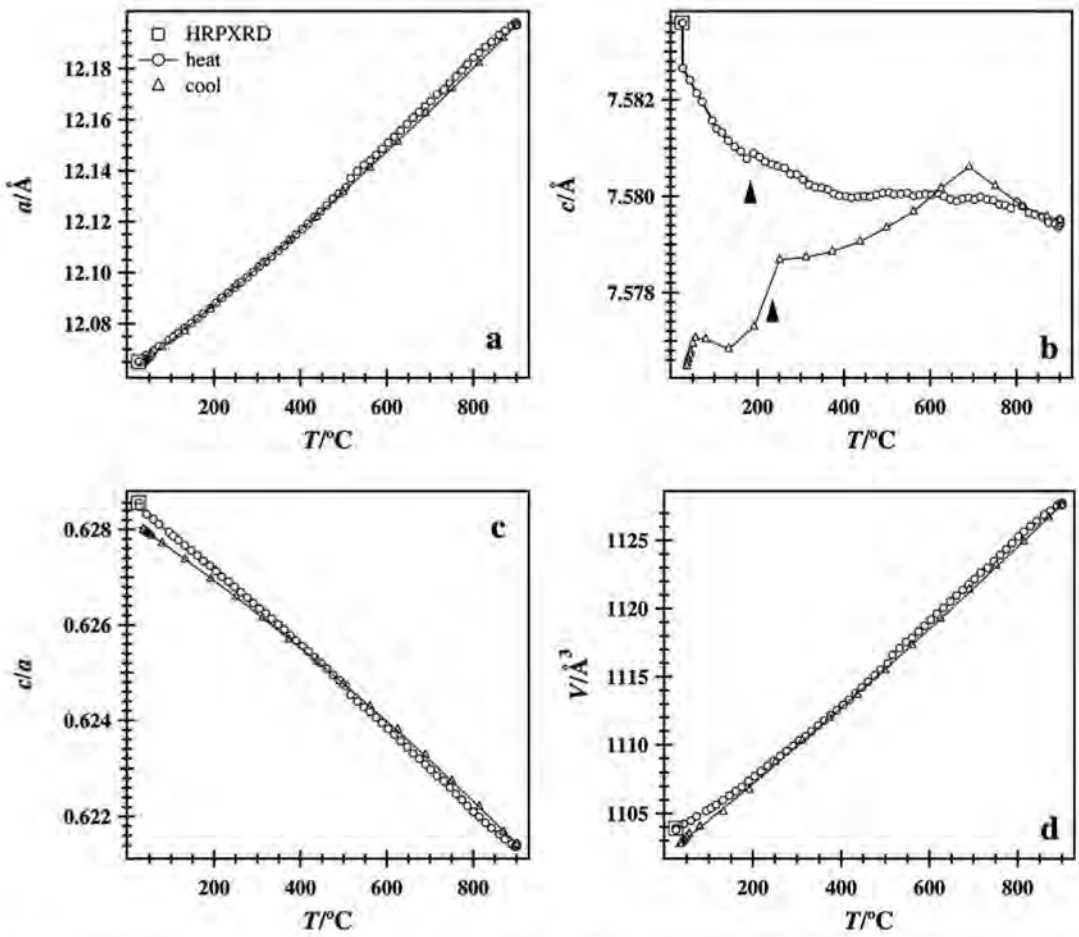

FIG. 5. Variation of unit-cell parameters with temperature. (a) a, (b) c, (c) ratio c/a, and (d) V. The HRPXRD data are displayed in the graphs. Smooth solid lines are polynomial fits that are used as guides for the eye. The fewer data points on cooling are also shown. Error bars, if not seen, are smaller than the symbols.

temperature. Furthermore, Al–Si order is not expected to change at 200°C.

Weak type-*b* reflections were observed in $Me_{79.6}$ using electron microscopy (Hassan & Buseck 1988), and Seto *et al.* (2004) observed type-*b* reflections and APBs in samples from Me_{18} to Me_{90}. Above Me_{75}, the type-*b* reflections may be explained by having inclusions of series 1 in a series-2 scapolite host (Hassan & Buseck 1988).

C–O distance and displacement parameters

The variation of the C–O7C distance with temperature is shown (Fig. 9c). The rigid CO_3 group is not expected to vary with T. The CO_3 group is positionally disordered, and a small amount of electron density occurs at the O7C site. Nevertheless, the C–O7C distance does vary in a systematic way and shows a break at 200°C. In $Me_{79.6}$, the C–O and S–O variations were found to be nearly constant to 900°C (Antao & Hassan 2008a).

The displacement parameters vary smoothly with temperature (Fig. 10). The T site has the smallest value, followed by the framework O atom, M cation, and anion groups. Large values occur for the anion groups because the CO_3 group is positionally disordered, and the M cations are disordered and bonded to these anion groups.

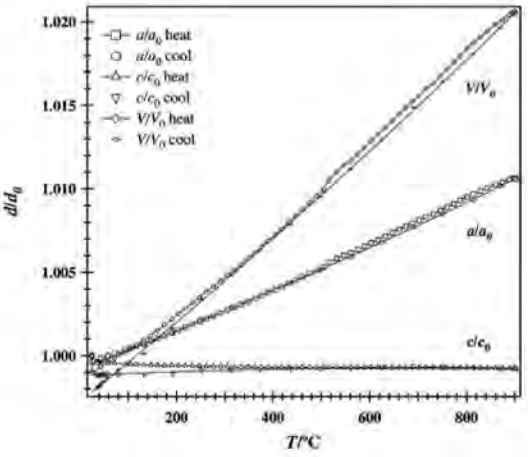

FIG. 6. Axial and volume expansion of the unit-cell parameters plotted with d/d_o as a function of T. The ratio c/c_o decreases slightly, whereas the a/a_o expansion is high.

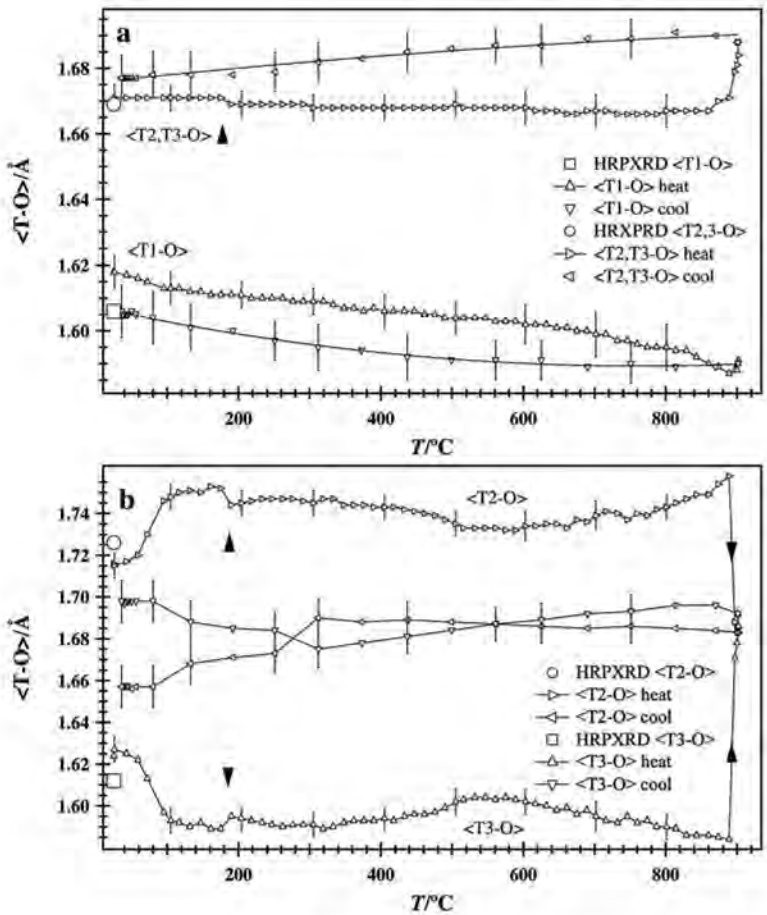

FIG. 7. Variation of average <T–O> distance with temperature. (a) <T1–O> and <T2,T3–O> distances, and (b) <T2–O> and <T3–O> distances. For the high-T data, error bars for only a few temperatures are shown for clarity.

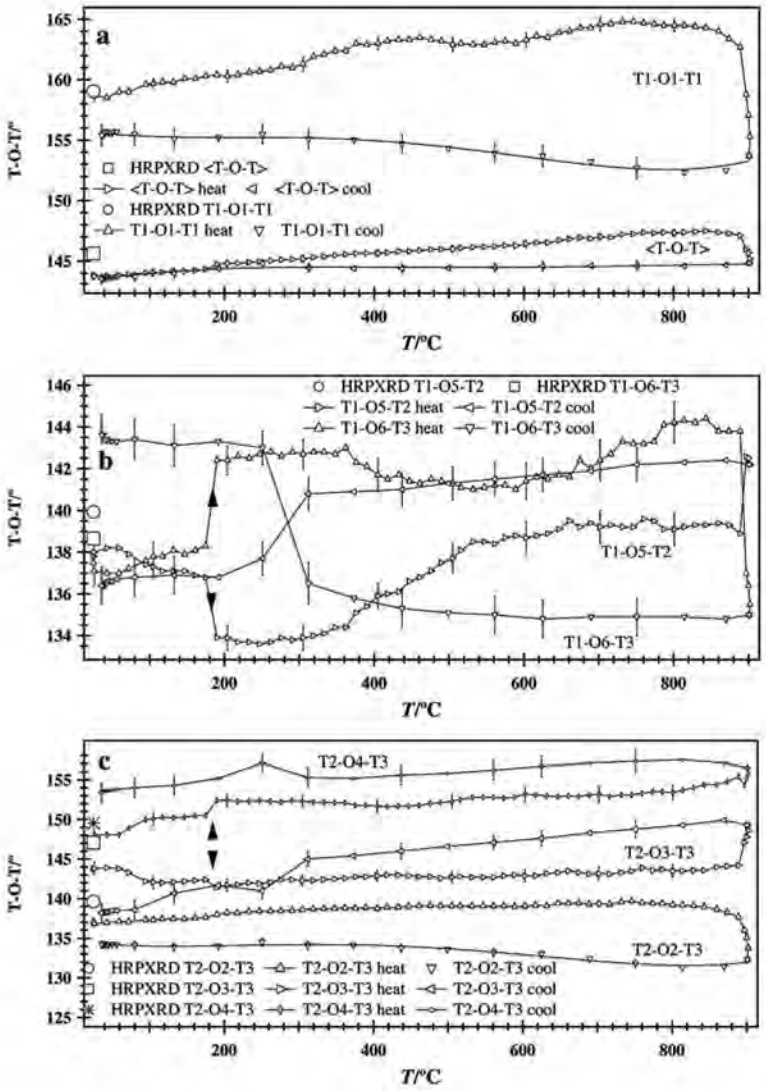

FIG. 8. Variation of bridging *T*–O–*T* angles with temperature. (a) *T*1–O1–*T*1 and <*T*–O–*T*>, (b) *T*1–O5–*T*2 and *T*1–O6–*T*3, and (c) *T*2–O4–*T*3, *T*2–O3–*T*3, and *T*2–O2–*T*3. Arrows point out changes at 200°C.

Oval channel

An oval channel is displayed at room temperature (Fig. 11). The long and short diameters are 9.386 and 3.291 Å at room temperature, and 9.364 and 3.615 Å at 902°C. The oval channel opens up as the short diameter increases with temperature (Fig. 12), as indicated by Levien & Papike (1976). A sharp increase in channel width occurs just before 200°C because of Na–Ca disorder, whereas a steep increase occurs near 900°C because of *T*2–*T*3 disorder.

The expansion of the scapolite structure occurs by increase in the <*M*–O> (and *M*–*A*) distances that cause the rigid TO_4 tetrahedra to rotate "out" (Fig. 9). Opening of the oval channels creates a more open framework structure (Figs. 11, 12). The <*M*–O> distance does not change significantly at 200°C, but the *M*–*A* distance and the *c* parameter increase (arrows in Figs. 5b, 9b), and the bridging angles, especially *T*1–O5–*T*2 and *T*1–O6–*T*3,

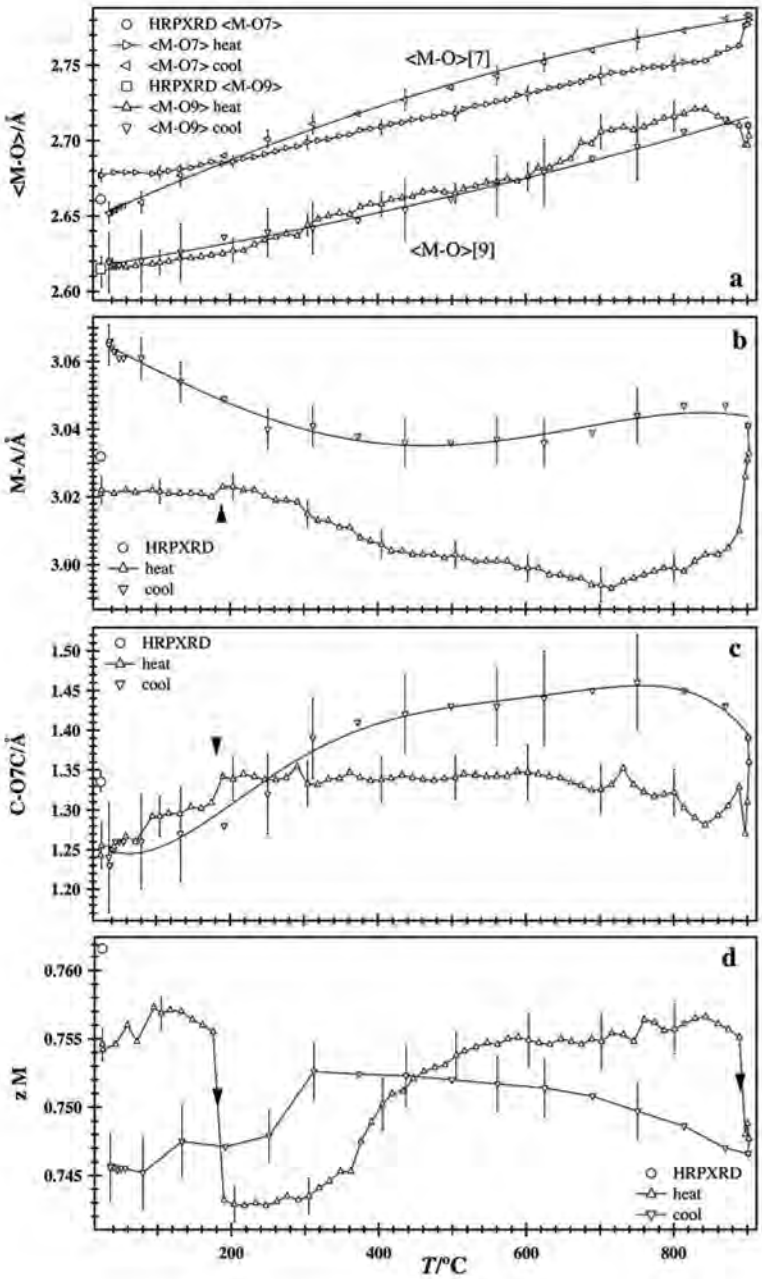

FIG. 9. Variations of (a) average <*M*–*O*>, (b) *M*–*A*, (c) C–O7C distances, and (d) *z* coordinate for the *M* site with temperature. Arrows point out changes at 200 and 900°C.

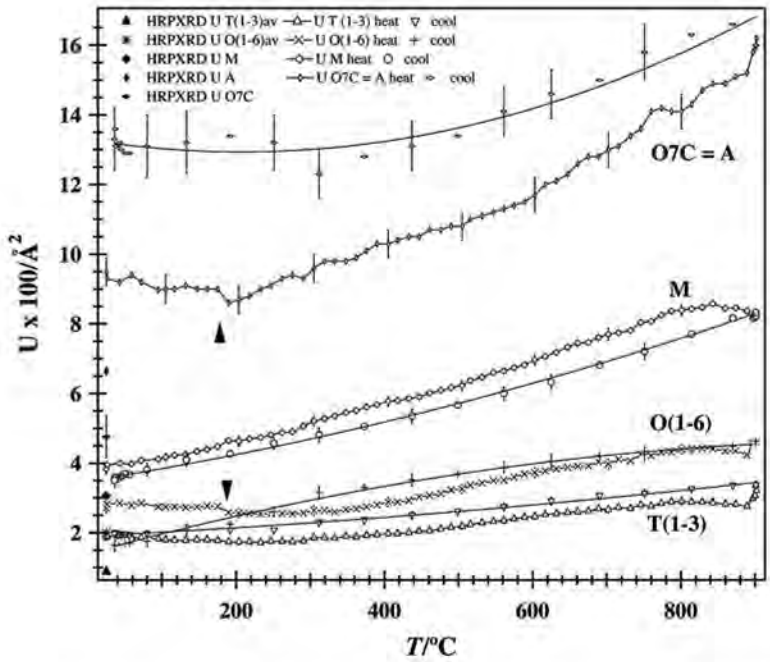

FIG. 10. Variation of isotropic displacement parameters, U, with temperature. For the IP data, the values of U decrease in the following order: $T(1–3) < O(1–6) < M << O7C = A$. Arrows point out changes at 200°C.

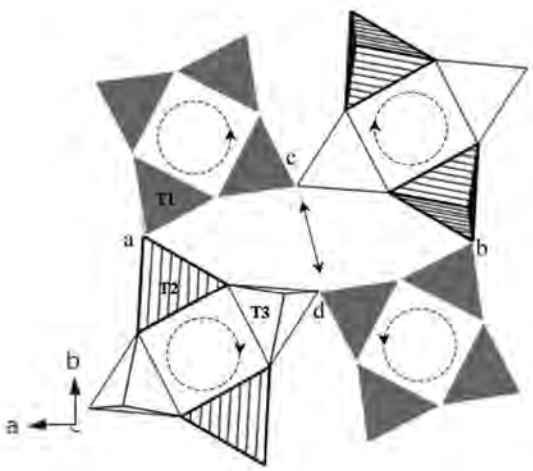

FIG. 11. Effect of thermal expansion on the rotation of tetrahedra and the oval channel in scapolite. Double-headed arrow indicates opening of the oval channel that arise from rotation of the TO_4 tetrahedra "out" as indicated by the arrows in the four-membered rings. These openings and rotations are caused by expansion of the <M–O> and M–A distances and give rise to a more open framework structure.

change (arrows in Fig. 8b). Therefore, the structural break at about 200°C reflects Na–Ca disorder, and gives rise to a slightly longer M–A distance (and constant <M–O> distance) that force the rigid TO_4 tetrahedra to rotate. The transition corresponding to Na–Ca disorder was also observed by differential scanning calorimetry (Antao & Hassan 2002). With increasing temperature, Na–Ca disorder near 200°C, the $T2$–$T3$ sites disorder near 900°C, and Cl–CO_3 anions remain ordered and give rise to APBs.

Seto *et al.* (2004) suggested that Me-rich scapolite, such as $Me_{79.6}$, is formed at high-temperature in space group $I4/m$; on rapid cooling, it may not change to space group $P4_2/n$ and remains metastably at room temperature, thereby implying that an I–P transition exists for scapolite. We did not observe any I–P transition in this study, nor in the study of $Me_{79.6}$ (Antao & Hassan 2008a).

CONCLUSIONS

All cell parameters increase continuously but nonlinearly with temperature, whereas the c parameter shows a break at 200°C. On cooling, the cell parameters, especially c, are not the same [c = 7.5836(2) Å before heating, and 7.5765(3) Å after cooling]. The average

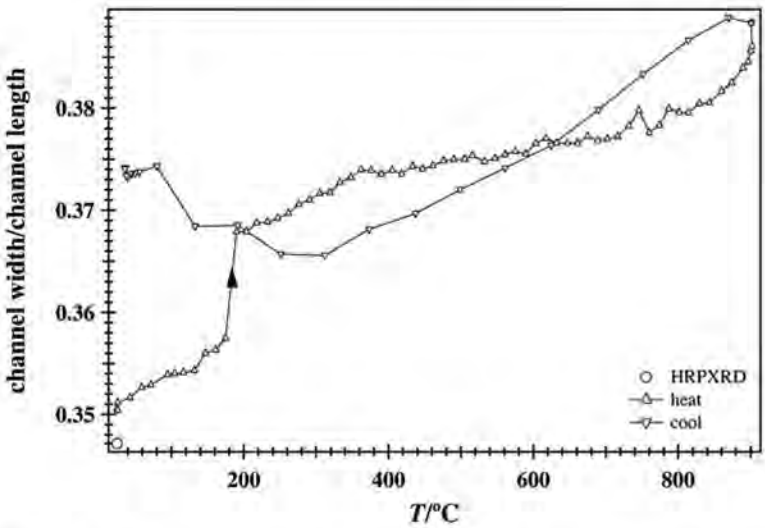

FIG. 12. Variation of the channel-width ratio (short axis O5c–O5d/long axis O6a–O6b) with temperature. This ratio shows a discontinuity between 175 and 190°C.

<*T*1–O>, <*T*2–O> and <*T*3–O>, 1.606(2), 1.726(2) and 1.612(2) Å in scapolite $Me_{32.9}$, correspond to the site occupancies *T*1 = $[Al_0Si_1]$, *T*2 = $[Al_{0.87}Si_{0.13}]$, and *T*3 = $[Al_{0.02}Si_{0.98}]$. At 902°C, <*T*1–O>, <*T*2–O> and <*T*3–O>, 1.591(5), 1.683(8) and 1.686(7) Å correspond to *T*1 = $[Al_0Si_1]$, *T*2 = $[Al_{0.55}Si_{0.45}]$, and *T*3 = $[Al_{0.57}Si_{0.43}]$. Therefore, at 902°C, the *T*1 site contains only Si atoms, whereas the *T*2–*T*3 sites are close to complete disorder. The quenched Al–Si and Na–Ca disorder gives rise to smaller values for the cell parameters on cooling. The Na–Ca disorder occurs at 200°C; several structural parameters show a break, including the *c* parameter. Disorder of the *M* cations causes the *M*–*A* distance to decrease, whereas the <*M*–O> distance increases, and forces the rigid TO_4 tetrahedra to rotate "out" and create a more open framework structure by expansion of the short diameter of the oval channel. Order of $[Na_4{\bullet}Cl]^{3+}$ and $[NaCa_3{\bullet}CO_3]^{5+}$ clusters occurs in series-1 scapolite (Hassan & Buseck 1988), and gives rise to considerable strain and APBs.

ACKNOWLEDGEMENTS

We dedicate this article to Joseph V. Smith in recognition of his important contributions to the mineralogy of framework silicates. We thank the two referees, R.B. Von Dreele and one anonymous, the Associate Editor, C.A. Geiger, and Editor, R.F. Martin, for useful comments. We thank B.H. Toby for his encouragement and support, and P.L. Lee for his help with the experiment. We thank Denis M. Shaw for providing the scapolite sample. The XRD data were collected at the X-ray Operations and Research beamlines 1–BM and 11–BM, APS, Argonne National Laboratory. Use of the APS was supported by the U.S. Department of Energy, Office of Science, Office of Basic Energy Sciences, under Contract No. DE–AC02–06CH11357.

REFERENCES

ANTAO, S.M. & HASSAN, I. (2002): Thermal behavior of scapolite $Me_{79.6}$ and $Me_{33.3}$. *Can. Mineral.* **40**, 1395-1401.

ANTAO, S.M. & HASSAN, I. (2008a): Unusual Al–Si ordering in calcic scapolite, $Me_{79.6}$, with increasing temperature. *Am. Mineral.* **93**, 1470-1477.

ANTAO, S.M. & HASSAN, I. (2008b): Gaudefroyite, $Ca_8Mn^{3+}{}_6[(BO_3)_6CO_3)_2O_6]$: high-temperature crystal structure. *Can. Mineral.* **46**, 183-193.

ANTAO, S.M. & HASSAN, I. (2008c): State-of-the-art high-resolution powder X-ray diffraction (HRPXRD) illustrated with Rietveld structure refinement of quartz, sodalite, tremolite, and scapolite $Me_{79.6}$. *Can. Mineral.* **46**, 1501-1509.

ANTAO, S.M., HASSAN, I., MULDER, W.H. & LEE, P.L. (2008): The $R\bar{3}c \rightarrow R\bar{3}m$ transition in nitratine, $NaNO_3$ and implications for calcite, $CaCO_3$. *Phys. Chem. Minerals* **35**, 545-557.

BAKER, J. (1994): Thermal expansion of scapolite. *Am. Mineral.* **79**, 878-884.

CHAMBERLAIN, C.P., DOCKA, J.A., POST, J.E. & BURNHAM, C.W. (1985): Scapolite: alkali atom configurations, antiphase domains, and compositional variations. *Am. Mineral.* **70**, 134-140.

DEER, W.A., HOWIE, R.A. & ZUSSMAN, J. (1992): *An Introduction to the Rock-Forming Minerals* (2nd ed.). John Wiley, New York, N.Y.

EVANS, B.W., SHAW, D.M. & HAUGHTON, D.R. (1969): Scapolite stoichiometry. *Contrib. Mineral. Petrol.* **24**, 293-305.

GRAZIANI, G. & LUCCHESI, S. (1982): The thermal behavior of scapolites. *Am. Mineral.* **67**, 1229-1241.

HASSAN, I., ANTAO, S.M. & PARISE, J.B. (2004): Sodalite: high-temperature structures obtained from synchrotron radiation and Rietveld refinements. *Am. Mineral.* **89**, 359-364.

HASSAN, I. & BUSECK, P.R. (1988): HRTEM characterization of scapolite solid solutions. *Am. Mineral.* **73**, 119-134.

HASSAN, I. & GRUNDY, H.D. (1984): The crystal-structures of sodalite-group minerals. *Acta Crystallogr.* **B40**, 6-13.

KABALOV, Y.K., SOKOLOVA, E.V., KALYGINA, N.V. & SCHNEIDER, J. (1999): Changes in the crystal structure of marialite during heating. *Crystallogr. Rep.* **44**, 979-983.

LARSON, A.C. & VON DREELE, R.B. (2000): General Structure Analysis System (GSAS). *Los Alamos National Lab., Rep.* **LAUR 86-748**.

LEVIEN, L. & PAPIKE, J.J. (1976): Scapolite crystal chemistry: aluminum–silicon distributions, carbonate group disorder, and thermal expansion. *Am. Mineral.* **61**, 864-877.

OTERDOOM, W.H. & WENK, H.-R. (1983): Ordering and composition of scapolite – field observations and structural interpretations. *Contrib. Mineral. Petrol.* **83**, 330-341.

PHAKEY, P.P. & GHOSE, S. (1972): Scapolite: observation of anti-phase domain structure. *Nature Phys. Sci.* **238**, 78-80.

RIETVELD, H.M. (1969): A profile refinement method for nuclear and magnetic structures. *J. Appl. Crystallogr.* **2**, 65-71.

SETO, Y., SHIMOBAYASHI, N., MIYAKE, A. & KITAMURA, M. (2004): Composition and $I4/m$–$P4_2/n$ phase transition in scapolite solid solutions. *Am. Mineral.* **89**, 257-265.

SHAW, D.M. (1960): The geochemistry of scapolite. I. Previous work and general mineralogy. *J. Petrol.* **1**, 218-260.

SHERRIFF, B.L., SOKOLOVA, E.V., KABALOV, Y.K., JENKINS, D.M., KUNATH-FANDREI, G., GOETZ, S., JÄGER, C. & SCHNEIDER, J. (2000): Meionite: Rietveld structure-refinement, ^{29}Si MAS and ^{27}Al SATRAS NMR spectroscopy, and comments on the marialite–meionite series. *Can. Mineral.* **38**, 1201-1213.

SHERRIFF, B.L., SOKOLOVA, E.V., KABALOV, Y.K., TEERTSTRA, D.K., KUNATH-FANDREI, G., GOETZ, S. & JÄGER, C. (1998): Intermediate scapolite: ^{29}Si MAS and ^{27}Al SATRAS NMR spectroscopy and Rietveld structure-refinement. *Can. Mineral.* **36**, 1267-1283.

SOKOLOVA, E.V., GOBECHIYA, E.R., ZOLOTAREV, A.A. & KABALOV, Y.K. (2000): Refinement of the crystal structures of two marialites from the Kukurt deposit of the east Pamirs. *Crystallogr. Reports* **45**, 934-938.

SOKOLOVA, E.V., KABALOV, Y.K., SHERRIFF, B.L., TEERTSTRA, D.K., JENKINS, D.M., KUNATH-FANDREI, G., GOETZ, S. & JÄGER, C. (1996): Marialite: Rietveld structure-refinement and ^{29}Si MAS and ^{27}Al satellite transition NMR spectroscopy. *Can. Mineral.* **34**, 1039-1050.

TEERTSTRA, D.K., SCHINDLER, M., SHERRIFF, B.L. & HAWTHORNE, F.C. (1999): Silvialite, a new sulfate-dominant member of the scapolite group with an Al–Si composition near the $I4/m$–$P4_2/n$ phase transition. *Mineral. Mag.* **63**, 321-329.

TEERTSTRA, D.K. & SHERRIFF, B.L. (1996): Scapolite cell-parameter trends along the solid-solution series. *Am. Mineral.* **81**, 169-180.

TOBY, B.H. (2001): EXPGUI, a graphical user interface for GSAS. *J. Appl. Crystallogr.* **34**, 210-213.

Received December 8, 2007, revised manuscript accepted August 26, 2008.